THE PUBLISHING HOUSE
OF THE ROMANIAN ACADEMY

PROCEEDINGS OF THE ROMANIAN ACADEMY, Series A,
Volume 24, Number 4/2023, pp. 349–359
DOI: 10.59277/PRA-SER.A.24.4.07

ANALYTICAL, NUMERICAL AND SCALE ANALYSIS STUDY OF THERMAL DIFFUSION EFFECT ON FREE CONVECTION BOUNDARY LAYER FLOWS IN A SLENDER POROUS LAYER

Mohammed ER-RAKI[1], Safae HASNAOUI[2], Mohammed HASNAOUI[2], Abderrahim BAZGAOU[1], Mohamed BOURICH[3]

[1] Cadi Ayyad University, Higher School of Technology, Essaouira, Morocco
[2] Cadi Ayyad University, LMFE, FSSM, Marrakesh, Morocco
[3] Cadi Ayyad University, National School of Applied Sciences, Marrakesh, Morocco
Corresponding author: Mohammed ER-RAKI, E-mail: m.erraki@uca.ac.ma

Abstract. This paper reports an analytical, numerical and scale analysis study of free convective heat and mass transfer flows coupled with thermal diffusion effect in a slender vertical porous cavity subjected to cooperating lateral temperature and concentration gradients. The top and bottom walls of the cavity are assumed to be adiabatic and impermeable to mass transfer. This study aims to analyze the different hydrodynamic, thermal and solutal behaviors developed in laminar boundary layer flow regime reached at high Rayleigh numbers. Based on the parallel flow approximation, an analytical solution of the problem is derived in the extreme case of heat-driven ($N \ll 1$) free convection. The obtained analytical results are validated numerically by generating the solutions of the full governing differential equations by means of finite-difference method (FDM). To estimate the order of magnitudes involved in the boundary layer regime, a scale analysis of the conservation equations is performed. The order of magnitudes of boundary layer thickness, Nusselt and Sherwood numbers are derived in this study. For all these quantities, the trends predicted by the scaling law theory are found to be in good agreement with those of the parallel flow approach. The combined effects of Rayleigh and Soret numbers on the boundary layer thickness, flow intensity and heat and mass transfers are illustrated graphically for representative values of N, Le and A_r, and the main results are highlighted and discussed.

Key words: heat and mass transfers, thermal diffusion phenomenon, boundary layer regime, parallel flow, scale analysis, numerical study.

1. INTRODUCTION

Thermal diffusion, commonly known as Soret effect, is one of the main mass transport phenomena that can occur in mixtures of mobile particles. It is a cross-transport process by which solutes can be transported in a multicomponent mixture under the effect of the applied temperature gradient [1–2]. This effect has aroused the attention of several researchers for a long time, and continues to do so. This interest rose from the occurrence of the phenomenon in many engineering applications and scientific systems, such as satellite problems, oil extractions, manufacturing of integrated circuits and many others. Details concerning the applications of the thermal diffusion in science and industry were given by Platten [3].

Experimentally, several efforts have been attempted on this subject despite the complexity of diffusion and thermal diffusion processes. It is to note here that, except some experimental tests devoted to analyse some specific behaviors [4, 5], most of these studies have addressed the measurement of the thermal diffusion coefficients of various multicomponent mixtures [6–9]. To this end, novel methods based on Thermogravitational [6], electrochemical impedance spectroscopy [7], thermal lens spectrometry [8] and microgravity [9] process have been presented and adopted in these studies. Recent experimental techniques used to simulate the thermal diffusion effect in binary and ternary liquid mixtures have been described and interpreted in the review conducted by Köhler *et al*. [10].

Despite its relevance and long history, the theoretical basis of the thermal diffusion effect on convective heat and mass transfer flows is still under debate. Previously, many theoretical studies [11−14] were conducted to investigate the thermal diffusion effect on the onset of the convective flows in porous enclosures with different configurations of heat and concentration gradients. All of these studies affirmed that the thermal diffusion effect could significantly affect the fluid flow, heat and mass transfer behaviors within the studied medium. Afterwards, many authors [15−18] followed similar paths to deal with various problems in the field. Er-Raki *et al*. [15] studied analytically and numerically the thermal diffusion effect on double diffusive natural convection in a horizontal Darcy porous enclosure heated and salted from the short sides. The study focused on the particular situation for which the rest state is a solution of the problem. Only the subcritical convection was found possible for this case and its threshold was determined analytically. Gaikwad and Kamble [16] studied theoretically the Soret effect on the onset of double diffusive rotating anisotropic convection in a horizontal sparsely packed porous layer. The effect of governing parameters of the problem on stationary and oscillatory convection was derived using linear stability theory based on the usual normal mode technique. Double diffusive natural convection in a differentially heated wavy cavity under thermophoresis (thermal diffusion) effect was studied numerically by Grosan *et al*. [17]. They showed that the effect of thermophoresis could be quite significant in appropriate situations and that the number of undulations could essentially modify the heat transfer rate and fluid flow intensity. More recently, Sarma and Ahmed [18] investigated the thermal diffusion effect on unsteady MHD free convective flow past a semi-infinite exponentially accelerated vertical plate in a porous medium. The influence of physical parameters on flow and transport characteristics was analyzed with suitable graphs. From the survey, it was observed that increasing the Soret number increased both the concentration and velocity fields.

The present work deals with a theoretical study of the effect of thermal diffusion on the free convection of heat and mass transfer in a porous enclosure subjected to cooperating horizontal gradients of temperature and concentration. The Darcy's fluid flow model is adopted in the momentum equation and the Boussinesq approximation is employed for the density variation. Thermal and solutal Neumann-type boundary conditions are applied on the active walls of the cavity. Parallel flow analytical solution is developed in steady state boundary layer regime in the extreme case of heat-driven ($N \ll 1$) natural convection. Scale analysis predictions of fluid flow and heat and mass transfer characteristics are also presented and compared with those of the parallel flow concept. The article ends by drawing some conclusions on the effects of both Rayeligh and Soret numbers on these fields for fixed values of the remaining governing parameters.

2. PROBLEM FORMULATION

The physical problem under study, depicted in Fig. 1, consists of a two-dimensional homogeneous, isotropic and saturated porous cavity of height H' and width L', filled with a binary fluid. The top and bottom end walls of the enclosure are adiabatic and impermeable to mass transfer while its lateral walls are subject to uniform fluxes of heat, q', and mass, j'. We assume here that the fluid saturating the matrix is Newtonian, and the flow is laminar, incompressible and obeys the Boussinesq approximation.

The Darcy's fluid flow model coupled with the energy and mass equations governing this problem can be written in a steady state as [12]:

$$\nabla^2\psi = -R_T\left(\frac{\partial T}{\partial x} + N\frac{\partial S}{\partial x}\right) \tag{1}$$

$$\nabla^2 T = u\frac{\partial T}{\partial x} + v\frac{\partial T}{\partial y} \tag{2}$$

$$\frac{1}{\mathrm{Le}}(\nabla^2 S + N_S\nabla^2 T) = u\frac{\partial S}{\partial x} + v\frac{\partial S}{\partial y} \tag{3}$$

$$u = \frac{\partial\psi}{\partial y}\,, \quad v = -\frac{\partial\psi}{\partial x}\,. \tag{4}$$

The appropriate boundary conditions are as follows:

$$\begin{cases} x = \pm\dfrac{1}{2} \ : \quad \psi = 0\,, \quad \dfrac{\partial T}{\partial x} = 1\,, \quad \dfrac{\partial S}{\partial x} = 1 - N_S \\ y = \pm\dfrac{A_r}{2} \ : \quad \psi = 0\,, \quad \dfrac{\partial T}{\partial y} = 0\,, \quad \dfrac{\partial S}{\partial y} = 0 \end{cases} \tag{5}$$

where ψ, T, S, u and v are the dimensionless stream function, temperature, concentration and horizontal and vertical components of flow velocity, respectively. In addition to these functions, four other dimensionless parameters appear in the governing equations, namely, the Soret number N_S, the thermal Rayleigh number R_T, the Lewis number Le and the solutal to thermal buoyancy ratio N, respectively.

The Nusselt and Sherwood numbers characterizing, respectively, the non-dimensional heat and mass transfer rates, across the vertical walls, are given by [12]:

$$\mathrm{Nu} = \frac{1}{T(1/2,\ 0) - T(-1/2,\ 0)} \qquad \text{and} \qquad \mathrm{Sh} = \frac{1}{S(1/2,\ 0) - S(-1/2,\ 0)} \tag{6}$$

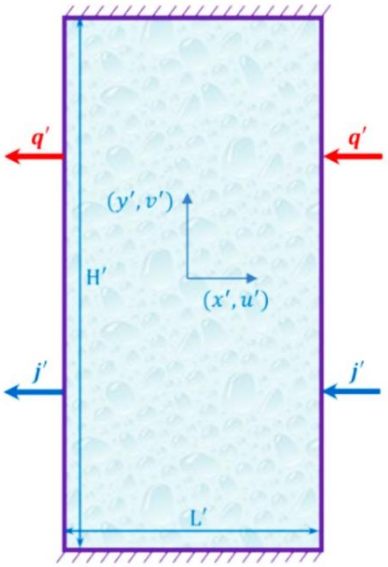

Fig. 1 – Physical configuration and coordinates system.

3. PROBLEM SOLUTION

3.1. Analytical solution

Due to the nonlinear coupling between the equations describing this problem, an exact analytical solution remains unavailable. However, in the limit of a shallow cavity ($A_r \gg 1$), an approximate solution of this equations model can be developed by adopting the following parallel flow assumptions which was successfully used in the past by Cormack et al. [19] and by many other authors after that for both fluid and porous media [12, 14, 15]:

$$\psi(x,y) \cong \psi(x)\,; \qquad T(x,y) \cong C_T y + \theta_T(x)\,; \qquad S(x,y) \cong C_S y + \theta_S(x) \tag{7}$$

where C_T and C_S are respectively unknown vertical temperature and concentration gradients. They can be determined by considering zero heat and mass transfers across any horizontal section of the enclosure [20]:

$$\int_{-1/2}^{1/2} \left(\frac{\partial \psi}{\partial x} T + \frac{\partial T}{\partial y}\right) \mathrm{d}x = 0 \qquad \text{and} \qquad \int_{-1/2}^{1/2} \left(\mathrm{Le}\frac{\partial \psi}{\partial x} S + \frac{\partial S}{\partial y} + N_S \frac{\partial T}{\partial y}\right) \mathrm{d}x = 0 \tag{8}$$

By introducing the approximations of equation (7) into governing equations of the problem, a system of classical differential equations is obtained. The boundary layer analytical solution of the resulting system

of equations with corresponding boundary conditions is given, at sufficiently small values of thermal to solutal buoyancy ratio ($N \ll 1$), as follows:

$$\psi(x) = \frac{1}{C_T}\left(1 - e^{\sqrt{R_T C_T}\left(|x|-\frac{1}{2}\right)}\right) \tag{9}$$

$$T(x,y) = C_T y + \frac{1}{\sqrt{R_T C_T}}\frac{|x|}{x} e^{\sqrt{R_T C_T}\left(|x|-\frac{1}{2}\right)} \tag{10}$$

$$S(x,y) = C_S y + \left(1 - \frac{\mathrm{Le} C_S}{C_T}\right)x + \frac{1}{\sqrt{R_T C_T}}\left(\frac{\mathrm{Le} C_S}{C_T} - N_S\right)\frac{|x|}{x} e^{\sqrt{R_T C_T}\left(|x|-\frac{1}{2}\right)} \tag{11}$$

where C_T and C_S represent the steady-state vertical temperature and concentration gradients, respectively. They can be expressed by computing the integrals of Equation (8), which leads to:

$$C_T \cong \frac{1}{\sqrt[5]{R_T}} \tag{12}$$

$$C_S \cong \frac{\mathrm{Le} C_T\left(\sqrt{R_T C_T} - 2\right) - N_S C_T\left(\mathrm{Le} + {C_T}^2\sqrt{R_T C_T}\right)}{\left({C_T}^2 + \mathrm{Le}^2\right)\sqrt{R_T C_T} - 3\mathrm{Le}^2} \tag{13}$$

Based on the criterion of horizontal velocities ratio at the boundary layer's edge, the boundary layer thickness, denoted by δx, can be approximately expressed as follows:

$$\delta x \cong \frac{1}{\sqrt{R_T C_T}} \cong \frac{1}{{R_T}^{2/5}} \tag{14}$$

The approximate expressions of Nusselt and Sherwood numbers can be given in boundary layer regime ($R_T \gg 1$) as follows:

$$\mathrm{Nu} \cong \frac{{R_T}^{2/5}}{2} \qquad \text{and} \qquad \mathrm{Sh} \cong \frac{{R_T}^{2/5}}{\left(1 - \frac{\mathrm{Le} C_S}{C_T}\right){R_T}^{2/5} + 2\left(\frac{\mathrm{Le} C_S}{C_T} - N_S\right)} \tag{15}$$

3.2. Numerical solution

To validate the parallel flow approximation adopted in the previous section, a numerical test allowing the resolution of the basic equations is carried out. The full equations (1)–(4) are solved using a classical central difference method. The iterative procedure is performed using the alternate direction implicit method (A.D.I.) for Eqs. (1), (2) and (3). In order to capture accurately the boundary layer profiles, a non-uniform grid, finer in the vicinity of the walls, is adopted. The computations reported in this paper were performed with a grid of 81×201 for A_r varying within the range $8 \le A_r \le 12$. To check the convergence of the numerical code, the criterion $\sum_i \sum_j \left|\Gamma_{i,j}^{n+1} - \Gamma_{i,j}^{n}\right| / \sum_i \sum_j \left|\Gamma_{i,j}^{n+1}\right| \le 10^{-5}$ is adopted.

3.3. Scale analysis solution

The aim of this section is to provide an approach based on scale analysis to estimate the orders of magnitude of the physical properties of the flowing fluid in the limiting case where the flow is dominated by thermal buoyancy forces ($N \ll 1$). This is the case where the force convection heat transfer is the dominant regime, and the density gradients are mainly induced by the temperature gradient due to lateral heating. In this analysis, we will specifically focus our attention on high Rayleigh number natural convection for which boundary layer type behaviors are observed for velocity, temperature and concentration profiles.

For this purpose, we need to rewrite our mathematical formulation in terms of velocities as follows:

$$\frac{\partial u}{\partial x} + \frac{\partial v}{\partial y} = 0 \tag{16}$$

$$\frac{\partial u}{\partial y}-\frac{\partial v}{\partial x}=-R_T\left(\frac{\partial T}{\partial x}+N\frac{\partial S}{\partial x}\right) \tag{17}$$

$$\left(\frac{\partial^2 T}{\partial x^2}+\frac{\partial^2 T}{\partial y^2}\right)=u\frac{\partial T}{\partial x}+v\frac{\partial T}{\partial y} \tag{18}$$

$$\frac{1}{\mathrm{Le}}\left(\frac{\partial^2 S}{\partial x^2}+\frac{\partial^2 S}{\partial y^2}\right)+\frac{N_S}{\mathrm{Le}}\left(\frac{\partial^2 T}{\partial x^2}+\frac{\partial^2 T}{\partial y^2}\right)=u\frac{\partial S}{\partial x}+v\frac{\partial S}{\partial y} \tag{19}$$

which is subjected to the following boundary conditions:

$$x=\pm\frac{1}{2}\ :\quad u=v=0\,,\quad \frac{\partial T}{\partial x}=1\,,\quad \frac{\partial S}{\partial x}=1-N_S \tag{20}$$

$$y=\pm\frac{A_r}{2}\ :\quad u=v=0\,,\quad \frac{\partial T}{\partial y}=0\,,\quad \frac{\partial S}{\partial y}=0\,. \tag{21}$$

According to Equations (17) and (18), the balances in terms of order of magnitude of the conservation equations momentum and energy in the vertical boundary region of thickness δx are given respectively by:

$$\frac{\delta v}{\delta x}\sim R_T\frac{\delta T}{\delta x} \tag{22}$$

$$C_T\delta v\sim\frac{\delta T}{\delta x^2} \tag{23}$$

where δv and δT are the vertical velocity and temperature boundary layers thicknesses, respectively, and C_T is the vertical gradient of the temperature in the enclosure (see Eq. (8)).

The order of magnitude scale relative to Equation (8) yields:

$$C_T\sim\delta v\,\delta T\delta x \tag{24}$$

In scaling terms, the thermal boundary condition imposed along the vertical boundaries (Eq. (20) implies:

$$\frac{\delta T}{\delta x}\sim 1 \tag{25}$$

The set of equations (22), (23), (24) and (25) can easily be solved to deduce the unknown scales for δx, δv, δT and C_T, which yields:

$$\delta x\sim {R_T}^{-2/5}\,;\quad \delta v\sim {R_T}^{3/5}\,;\quad \delta T\sim {R_T}^{-2/5}\,;\quad C_T\sim {R_T}^{-1/5} \tag{26}$$

The heat transfer rate is then scaled as:

$$\mathrm{Nu}\sim\frac{1}{\delta T}\sim {R_T}^{2/5} \tag{27}$$

At sufficiently high thermal Rayleigh numbers, a boundary layer, of thickness δy, develops along the top and bottom walls of the cavity. Let δu and $\overline{\delta T}$ be the horizontal velocity and temperature changes across this layer. The orders of magnitude deduced form the conservation equations of mass, momentum and energy in a horizontal region of thickness δy are given respectively by:

$$\delta u\delta y\sim\delta v\delta x \tag{28}$$

$$\frac{\delta u}{\delta y}\sim R_T\delta T \tag{29}$$

$$\frac{\overline{\delta T}}{\delta y^2}\sim\delta u\delta T \tag{30}$$

Upon combining the results of (26) with the equations (28), (29) and (30), we find that:

$$\delta y \sim {R_T}^{-1/5}\,; \qquad \delta u \sim {R_T}^{2/5}\,; \qquad \overline{\delta T} \sim {R_T}^{-2/5} \tag{31}$$

Referring to Eq. (19), the scale of concentration changes across the vertical boundary layer depends on the Lewis number Le (ratio of molecular heat to mass diffusivity). It is therefore necessary to consider separately whether the mass transfer is ruled by convection ($\mathrm{Le} \gg 1$) or by diffusion ($\mathrm{Le} \ll 1$).

3.3.1. Convective mass transfer ($\mathbf{Le} \gg \mathbf{1}$)

It is relevant to note here that in the absence of thermal diffusion effect ($N_S = 0$), the vertical concentration boundary layer has the same thickness as both the hydrodynamic and the thermal ones ($\delta S \sim \delta T \sim \delta x$). When taking the thermal diffusion effect into account, the boundary layer thickness of the concentration profile is found to be proportional to the hydrodynamic one ($\delta S \sim (1 - N_S)\delta x$) and the coefficient of proportionality is a function of the Soret number, N_S.

In scaling terms, the solutal boundary conditions imposed along the vertical sides, Eq. (20), yields:

$$\frac{\delta S}{\delta x} \sim 1 - N_S \tag{32}$$

In a vertical boundary layer of thickness δx, the conservation equation of species Eq. (19) allows us to write:

$$C_S \delta v \sim \left(\frac{1}{\mathrm{Le}}\frac{\delta S}{\delta x^2}\right); \quad \left(\frac{N_S}{\mathrm{Le}}\frac{\delta T}{\delta x^2}\right) \tag{33}$$

with C_S being the vertical concentration gradient.

The three terms of the equation (33) are therefore balanced. To determine the appropriate order of magnitude of C_S, one must discuss the two extreme cases of large and small values of the Soret number, N_S. For sufficiently large values of N_S ($N_S \gg 1$) , the equation (33) reduces to:

$$C_S \delta v \sim \left(\frac{N_S}{\mathrm{Le}}\frac{\delta T}{\delta x^2}\right) \tag{34}$$

Using Eqs. (26) and (34), we obtain:

$$C_S \sim \frac{N_S}{\mathrm{Le}} {R_T}^{-1/5} \tag{35}$$

For sufficiently small values of N_S ($N_S \ll 1$), the equation (33) gives:

$$C_S \delta v \sim \frac{1}{\mathrm{Le}}\frac{\delta S}{\delta x^2} \tag{36}$$

Upon combining the equations (26), (32) and (36), we obtain:

$$C_S \sim \frac{1}{\mathrm{Le}} {R_T}^{-1/5} \tag{37}$$

For both cases, the scale of the Sherwood number is such that:

$$\mathrm{Sh} \sim \frac{1}{\delta S} \sim \frac{1}{1 - N_S} {R_T}^{2/5} \tag{38}$$

3.3.2. Diffusive mass transfer ($\mathbf{Le} \ll \mathbf{1}$)

For this situation, no boundary layer behavior is observed for the concentration profile. This result can be deducted from the iso-concentrations presented in Fig. 2 where the contour lines are found practically parallel to the long vertical walls. The mass transfer is then ruled essentially by diffusion.

The horizontal concentration drop over the width of the cavity is given in this case as follows:

$$\delta S \sim\ 1 - 2N_S {R_T}^{-2/5} \tag{39}$$

The transfer of mass is that of pure diffusion and the Sherwood number is scaled as:

$$\mathrm{Sh} \sim \frac{{R_T}^{2/5}}{{R_T}^{2/5} - 2N_S}, \tag{40}$$

which corresponds, in the absence of thermal diffusion effect, to a Sherwood number of O(1) or Sh ~ 1.

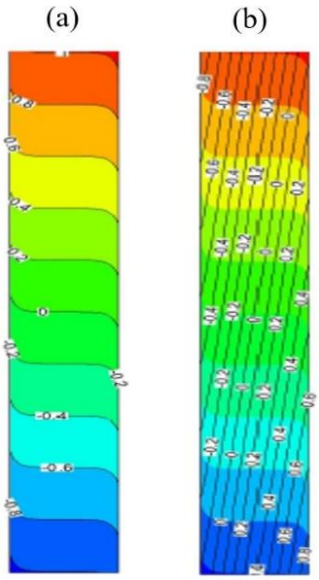

Fig. 2 – Isotherms (a) and iso-concentrations (b) contours obtained for $R_T = 10^3$, $N = 10^{-4}$, Le $= 10^{-3}$, $N_S = 0.4$ and $A_r = 8$.

4. RESULTS AND DISCUSSION

In this section, the most interesting results for both analytical and numerical methods are reported and discussed, and the combined effects of the governing parameters on the fluid flow properties and heat and mass transfer characteristics are illustrated and analyzed.

Aiming to render the problem amenable to a very helpful parametric study, an analytical solution of the governing equations is proposed based on the parallel flow approximation valid in the case of a shallow cavity. To confirm the validity of this approach, the study is completed by a numerical simulation of the full governing equations of the problem based on a second-order finite difference scheme. Typical numerical results, in terms of streamlines (a), isotherms (b) and iso-concentrations (c), are presented in Fig. 3 for N_S = 0.5, Le = 3, N = 10^{-3}, R_T = 10 and A_r = 8. The fundamental character of the parallel flow approach is well illustrated in this figure. Thus, it can be seen from this figure that the velocity is parallel to the long boundaries in the core region of the cavity and the temperature and concentration profiles are linearly stratified in the vertical direction. Taken together, these findings strongly confirm the reliability and validity of the parallel flow assumptions adopted in this study to develop an analytical solution for the problem.

Given its specific physical characteristics, attention is focused on the boundary layer regime which is found to exist for sufficiently large values of Rayleigh number. The scope of this study is restricted to the identification and analysis of boundary layer behaviors developed by double diffusion in the extreme case of heat-driven ($N \ll 1$) natural convection. We limit ourselves here to highlighting high Rayleigh number natural convection for which boundary layer type behaviors are observed for velocity, temperature and concentration profiles. This specific behavior can be clearly seen in Fig. 4 which displays the horizontal profiles of temperature, concentration and velocity at the mid-height of the enclosure for a given combination of governing parameters. Both analytical and numerical results are presented and the agreement between the two predictions can be clearly observed. It is obvious from the plots depicted in this figure that the horizontal gradients of temperature, concentration and velocity are nearly zero outside the vertical boundary layers (the boundary layer regime character).

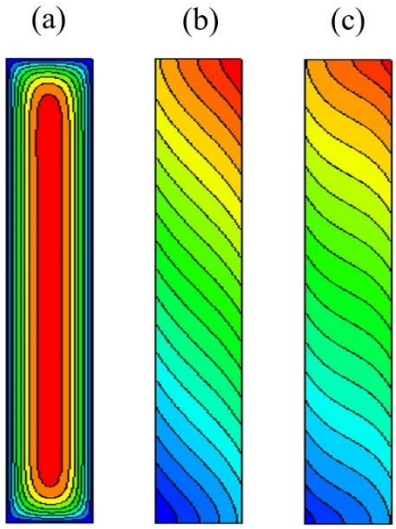

Fig. 3 – Streamlines (a), isotherms (b) and iso-concentrations (c) contours obtained for $N_S = 0.5$, Le $= 3$, $N = 10^{-3}$, $R_T = 10$ and $A_r = 8$.

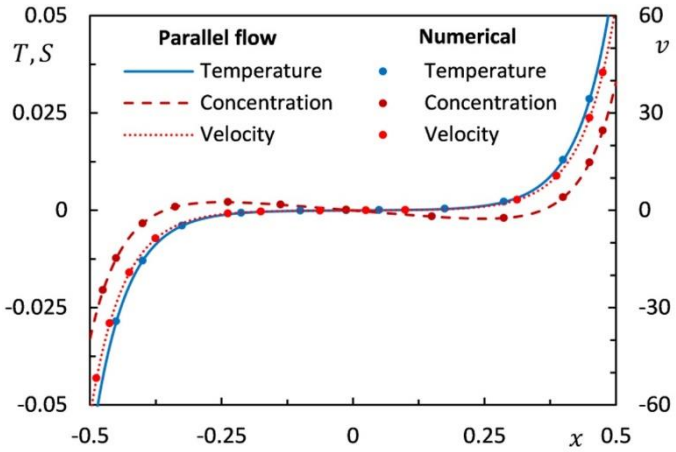

Fig. 4 – Horizontal profiles of temperature, concentration and velocity at the mid-height of the enclosure for $R_T = 10^3$, $N = 10^{-4}$, Le $= 2$, $N_S = 0.4$ and $A_r = 8$.

After having validated the parallel flow results numerically, let us now highlight these results and compare them with those of scale analysis. In view of the approximate solutions developed above, it clearly appears that there is excellent agreement between the expressions derived on the basis of the parallel flow concept and those obtained by scale analysis. More specifically and referring to equations (12) to (15) and equations (26) and (27), the vertical temperature gradient, C_T, the boundary layer thickness, δx, and the Nusselt number, Nu, are found for both theories to be varied as ${R_T}^{-1/5}$, ${R_T}^{-2/5}$ and ${R_T}^{2/5}$, respectively. As for the concentration profile, both approaches also showed, with the same tendency, that the scale of concentration changes across the vertical boundary layer depends on the Lewis, Le, and Soret, N_S, numbers. In this regard and in order to estimate the order of magnitude of the Sherwood number, representing this profile, the two extreme cases of convective (Le $\gg 1$) and diffusive (Le $\ll 1$) mass transfer are separately examined and the corresponding predictions are reported. As can be seen from equations (15) and (40), the degree of agreement of the analytical predictions and scale analysis is seen to be good.

By comparing the results of equations (26) and (31), it can be clearly seen that the horizontal boundary layer is thicker than the vertical one. These equations also allow us to deduce that the velocity changes through the vertical boundary layer are larger than those observed in the horizontal one. Another significant result that emerges from this analysis is that the temperature changes through both the horizontal and vertical boundary layers have the same amplitude, both vary as ${R_T}^{-2/5}$.

We now turn our attention to the effect of R_T on the fluid flow and heat and mass transfer characteristics inside the cavity for given values of the pertinent flow parameters N, Le and N_S. The variations with R_T of the boundary layer thickness, δx, the stream function at the center of the enclosure, ψ_0, the Nusselt, Nu, and Sherwood, Sh, numbers are illustrated, respectively, in Figs. (5)–(8) for $N = 10^{-3}$ (heat-driven flow), $\mathrm{Le} = 3$ and different values of Soret number, N_S. Firstly, it is clearly seen from these figures that the parallel flow predictions represented by solid lines are in excellent agreement with the fully numerical results depicted by dotted lines, thus demonstrating the validity of the parallel flow approximation adopted in this study. Likewise, and as anticipated, these plots show that the boundary layer analytical results agreed well with the parallel flow ones for relatively high values of R_T, which justifies the simplifications performed above to find a solution to the problem in boundary layer regime. The critical values of R_T beyond which the boundary layer regime is reached differ from one characteristic function to another and are independent of the Soret parameter. Furthermore, these figures also illustrate that as Rayleigh number increases, the Nusselt number and stream function increase as well, while the vertical boundary layer thickness decreases monotonically. These trends are in agreement with the analytical predictions, where Nu, ψ_0 and δx varied according to ${R_T}^{2/5}$, ${R_T}^{1/5}$ and ${R_T}^{-2/5}$, respectively. In contrast, and as expected, the mass transfer, characterized by Sherwood number and depicted in Fig. 8, is seen to be strongly affected by the Soret number. It was found positive in both cases $N_S = -5$ and $N_S = 0$ (without Soret effect) and negative for $N_S = 5$, which is consistent with equations (15) and (38). These results prove that the Soret effect plays a significant role in concentration diffusion between the vertical walls of the medium. Another result obtained from this study is that, at low Rayleigh numbers, heat transfer is dominated by his pure diffusive regime ($\psi_0 \cong 0, \mathrm{Nu} \cong 1$) regardless of the Soret effect.

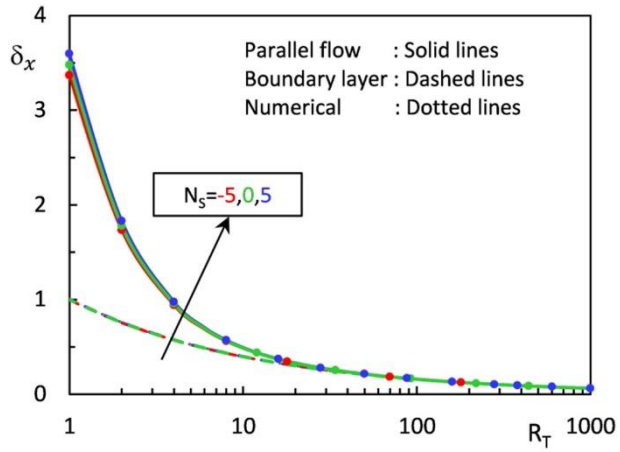

Fig. 5 – Effect of R_T on δx for $N = 10^{-3}$, $\mathrm{Le} = 3$, $A_r = 8$ and different values of N_S.

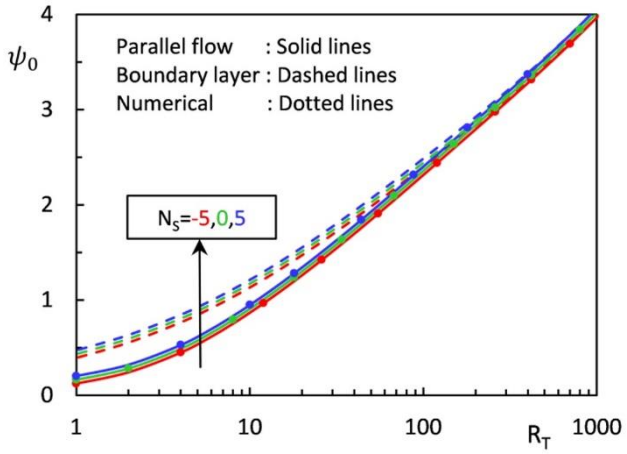

Fig. 6 – Effect of R_T on ψ_0 for $N = 10^{-3}$, $\mathrm{Le} = 3$, $A_r = 8$ and different values of N_S.

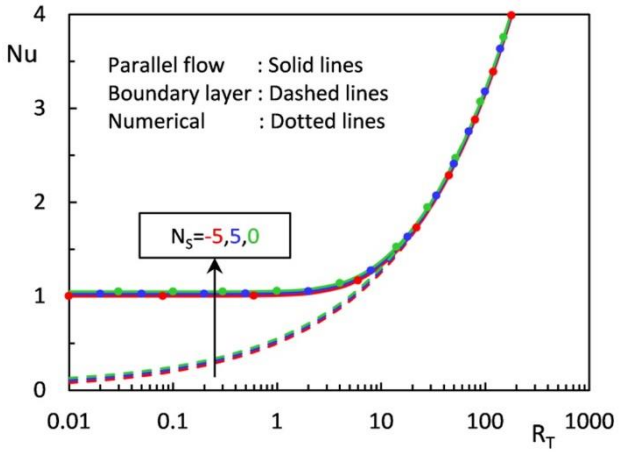

Fig. 7 – Effect of R_T on Nu for $N = 10^{-3}$, $\mathrm{Le} = 3$, $A_r = 8$ and different values of N_S.

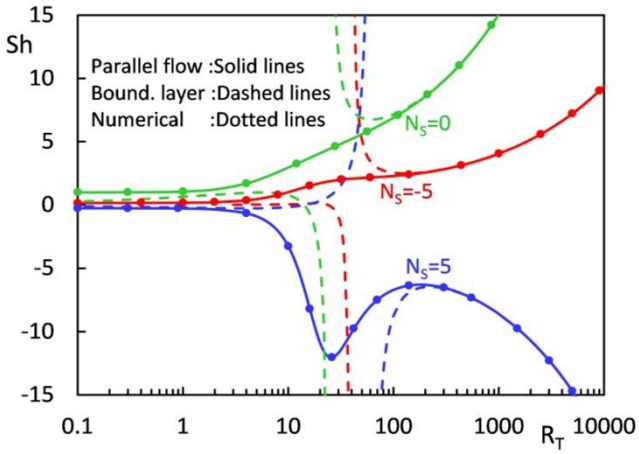

Fig. 8 – Effect of R_T on Sh for $N = 10^{-3}$, $\mathrm{Le} = 3$, $A_r = 8$ and different values of N_S.

5. CONCLUSION

Thermal diffusion effect on free convective heat and mass transfer within a vertical porous enclosure submitted to horizontal temperature and concentration gradients is studied analytically and numerically. The study is mainly devoted to the analysis of fluid flow, heat and mass transfer processes in boundary layer convective flows within a cavity saturated by a binary mixture. Of particular interest of this study is to examine the different boundary layer behaviors developed in the limiting case where the flow is dominated by thermal buoyancy forces ($N \ll 1$). An approximate analytical solution of the problem, valid for shallow enclosures, is derived on the basis of the parallel flow assumptions and validated numerically by solving the full governing equations. In this paper is also presented a scale analysis development used to estimate the fluid flow and heat and mass transfer characteristics order of magnitudes. A good agreement between the scale analysis results and those of parallel flow assumptions was found. Relevant to this study, results showed that the vertical hydrodynamic and thermal boundary layers thicknesses are equivalent $\left(\delta x \sim \delta T \sim {R_T}^{-2/5}\right)$ and that the Nusselt number varies as ${R_T}^{2/5}$ regardless of the Soret number, N_S. The mass transfer characteristics inside the enclosure, on the contrary, are found to be strongly affected by the thermal diffusion effect. Indeed, the concentration boundary layer thickness and Sherwood number were found to vary, respectively, as $\delta S \sim (1 - N_S){R_T}^{-2/5}$ and $\mathrm{Sh} \sim \frac{1}{1-N_S}{R_T}^{2/5}$ for $\mathrm{Le} \gg 1$ and $\delta S \sim 1 - 2N_S{R_T}^{-2/5}$ and $\mathrm{Sh} \sim \frac{{R_T}^{2/5}}{{R_T}^{2/5} - 2N_S}$ for $\mathrm{Le} \ll 1$. For this last case, it was also found that no boundary layer behavior is observed for the concentration profile and, therefore, mass transfer is mainly governed by diffusion.

REFERENCES

1. A.J. CHAMKHA, S.M.M. EL-KABEIR, *Unsteady heat and mass transfer by MHD mixed convection flow over an impulsively stretched vertical surface with chemical reaction and Soret and Dufour Effects*, Chemical Engineering Communications, **200**, pp. 1220–1236, 2013.
2. M.A. RAHMAN, M.Z. SAGHIR, *Thermodiffusion or Soret effect: Historical review*, International Journal of Heat and Mass Transfer, **73**, pp. 693–705, 2014.
3. J.K. PLATTEN, *The Soret effect: a review of recent experimental results*, Journal of Applied Mechanics, **73**, *1*, pp. 5–15, 2006.
4. M. ALMASI, S. HEYDARIAN, *Thermal behavior and Soret effect in methyl phenyl ketone and 2-alkanol mixtures*, Journal of Molecular Liquids, **344**, art. 117934, 2021.
5. B. ŠETA, J. GAVALDA, M.M. BOU-ALI, X. RUIZ, *Stability analysis under thermogravitational effect*, International Journal of Thermal Sciences, **156**, art. 106464, 2020.
6. B. ŠETA, J. GAVALDA, M.M. BOU-ALI, X. RUIZ, C. SANTAMARIA, *Determining diffusion, thermodiffusion and Soret coefficients by the thermogravitational technique in binary mixtures with optical digital interferometry analysis*, International Journal of Heat and Mass Transfer, **147**, art. 118935, 2020.
7. M. JOKINEN, J. MANZANARES, L. MURTOMÄKI, *Soret coefficient of trace ions determined with electrochemical impedance spectroscopy in a thin cell. Theory and measurement*, Journal of Electroanalytical Chemistry, **820**, pp. 67–73. 2018.
8. H. CABRERA, F. CORDIDO, A. VELÁSQUEZ, P. MORENO, E. SIRA, S.A. LÓPEZ-RIVERA, *Measurement of the Soret coefficients in organic/water mixtures by thermal lens spectrometry*, Comptes Rendus Mécanique, **341**, *4–5*, pp. 372–377, 2013.
9. A. MOJTABI, *A new process for the determination of the Soret coefficient of a binary mixture under microgravity*, International Journal of Thermal Sciences, **149**, art. 106204, 2020.
10. W. KÖHLER, K.I. MOROZOV, *The Soret effect in liquid mixtures – A Review*, Journal of Non-Equilibrium Thermodynamics, **41**, *3*, pp. 151–197, 2016.
11. A. BAHLOUL, N. BOUTANA, P. VASSEUR, *Double-diffusive and Soret-induced convection in a shallow horizontal porous layer*, Journal of Fluid Mechanics, **491**, pp. 325–352, 2003.
12. R. BENNACER, A. MAHIDJIBA, P. VASSEUR, H. BEJI, R. DUVAL, *The Soret effect on convection in a horizontal porous domain under cross temperature and concentration gradients*, International Journal of Numerical Methods for Heat and Fluid Flow, **13**, *2–3*, pp. 199–215, 2003.
13. M. BOURICH, M. HASNAOUI, M. MAMOU, A. AMAHMID, *Soret effect inducing subcritical and Hopf bifurcations in a shallow enclosure filled with a clear binary fluid or a saturated porous medium: A comparative study*, Physics of Fluids, **16**, *3*, pp. 551–568, 2004.
14. M. ER-RAKI, M. HASNAOUI, A. AMAHMID, M. BOURICH, *Soret driven thermosolutal convection in a shallow porous layer with a stress-free upper surface*, Engineering Computations, **22**, pp. 186–205, 2005.

15. M. ER-RAKI, M. HASNAOUI, A. AMAHMID, M. BOURICH, *Subcritical convection in the presence of Soret effect within a horizontal porous enclosure heated and salted from the short sides*, International Journal of Numerical Methods for Heat and Fluid Flow, **21**, pp. 150–167, 2011.
16. S.N. GAIKWAD, S.S. KAMBLE, *Linear stability analysis of double diffusive convection in a horizontal sparsely packed rotating anisotropic porous layer in presence of Soret effect*, Journal of Applied Fluid Mechanics, **7**, pp. 459–471, 2014.
17. T. GROSAN, M.A. SHEREMET, I. POP, S.R. POP, *Double-diffusive natural convection in a differentially heated wavy cavity under thermophoresis effect*, Journal of Thermophysics and Heat Transfer, **32**, *5*, pp. 1–14, 2018.
18. S. SARMA, N. AHMED, *Thermal diffusion effect on unsteady MHD free convective flow past a semi-infinite exponentially accelerated vertical plate in a porous medium*, Canadian Journal of Physics, **100**, *10*, pp. 437–451, 2022.
19. D.E. CORMACK, L.G. LEAL, J. IMBERGER, *Natural convection in a shallow cavity with differentially heated end walls. Part 1. Asymptotic theory*, Journal of Fluid Mechanics, **65**, *2*, pp. 209–229, 1974.
20. O.V. TREVISAN, A. MOSTA, *Mass and heat transfer by natural convection in a vertical slot filled with porous medium*, International Journal of Heat and Mass Transfer, **29**, *3*, pp. 403–415, 1986.

Received on February 16, 2023